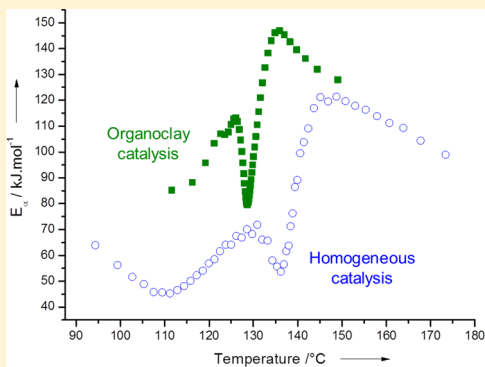


Complex Kinetic Pathway of Furfuryl Alcohol Polymerization Catalyzed by Green Montmorillonite Clays

Raffaele Zavaglia, Nathanael Guigo,* Nicolas Sbirrazzuoli, Alice Mija, and Luc Vincent

Fluids and Complex Materials Group, Laboratory of Condensed Matter Physics (L.P.M.C – UMR 7336), University of Nice - Sophia Antipolis, 06108 Nice Cedex 2, France

ABSTRACT: Furfuryl alcohol (FA) which is derived from lignocellulosic biomass polymerizes into poly(furfuryl alcohol) (PFA) under acidic catalysis. A greener and more sustainable catalytic route was proposed in order to replace hazardous acidic catalysts. Organically modified montmorillonite (Org-MMT) and, in comparison, sodium MMT (Na-MMT) are used to evaluate the catalytic effect on the FA polymerization. X-ray diffraction (XRD) and transmission electronic microscopy (TEM) show that clay layers have been exfoliated during polymerization. Additional FTIR spectroscopy measurements confirm that furanic oligomers have intercalated between clay layers by cation exchange. An original combination between chemorheological and model-free kinetic analysis allows highlighting the influence of MMT on the overall polymerization pathway. The octadecyl ammonium cation (ODA) was also used as homogeneous acidic catalyst to highlight the specific role of this interlayer cation present in Org-MMT. Interestingly, FA/Org-MMT polymerizes more rapidly than FA/ODA but initiation of polymerization is slightly shifted to higher temperature due to initial intercalation between MMT layers. Then, the dual acidic character (Lewis + Brønsted) of Org-MMT leads to gelation at early stage of polymerization. The results clearly show that exfoliation of MMT layers increases the efficiency of collisions.



1. INTRODUCTION

For years, research in polymer science has focused on finding alternative sources of monomers and greener polymerization routes. The use of biomass-based building blocks as replacement of oil-based chemicals represents a sustainable solution for the development of new commodity materials.¹ However, the use of raw materials derived from starch or sugar is strongly debated, because these feedstocks could be used for food applications. Among the promising and sustainable biomass-based derivatives, furfural is obtained from pentose-rich agro waste streams, i.e., from nonfood crop processing. Most of the furfural produced worldwide is derivatized into furfuryl alcohol (FA) by a selective hydrogenation process.² Under either Brønsted or Lewis acidic catalysis, FA polymerizes into poly(furfuryl alcohol) (PFA).^{3,4} This biomass-based furanic thermoset is widely used in several applications such as for foundry molds,⁵ precursors to carbonaceous products,⁶ wood modification,^{7–9} wood adhesives,¹⁰ and polymer composites.¹¹ The reported step-growth curing mechanisms of FA can be separated into two stages. First, the hydroxymethyl group of FA condenses on the C₅ position of another furan ring leading to linear oligomers connected by methylene linkages.¹² In a second stage, these linear oligomers are cross-linked into branched black materials. Formation of chromophores were demonstrated by NMR experiments¹³ and the authors postulated that cross-linking reactions occur via either electrophilic addition on conjugated sequences or Diels–Alder cycloaddition between furan ring (diene) and dihydrofuranic cycles (dienophile). The theoretical modeling

studies conducted by Montero et al.¹⁴ showed that cyclo-addition is possible from a frontier molecular orbital point of view, but the high steric hindrance has a negative contribution. On the contrary, electrophilic addition is more consistent and likely to occur preferentially. Concerning polymerization catalysts, the activity of mineral acids (phosphoric acid,¹⁵ sulfuric acid¹⁶), organic acids (*p*-toluene sulfonic acid,^{17,18} maleic anhydride,^{15,19} trifluoroacetic acid^{20,21}), Lewis acid (TiCl₄,¹³ SnCl₄,¹³ ZnCl₂²²), and iodine^{23,24} was evaluated. Most of these catalysts are not safe for the environment.

Smectites clays such as montmorillonite (MMT) are considered as selective, safe, efficient, and eco-friendly catalysts that meet the requirements of green chemistry concerns.²⁵ MMT is layered aluminosilicate where the silica tetrahedra are bonded with alumina octahedra to form a sheet-like structure. Within the interlayer spaces, charge compensating counterions (K⁺, Na⁺, Ca²⁺, and so on) are located to render clays hydrophilic. The above-mentioned alkali or alkali-earth cations can be exchanged with metallic cations²⁶ (Al³⁺, Ti⁴⁺, Fe³⁺, Cu²⁺) or organic cations²⁷ (generally alkyl-ammonium). In the latter case, the organically modified layered silicates present improved wetting characteristics with the hydrophobic solvent or polymer. Natural MMT might play a role in origins of life²⁸ because it can act as a prebiotic catalyst in the formation of RNA oligomers. Nowadays, MMT are widely used in chemical

Received: February 13, 2012

Revised: June 13, 2012

Published: June 15, 2012

engineering as high-performance heterogeneous solid catalysts. It is noteworthy that MMT exhibits both Brönsted and Lewis acid sites. The Brönsted acidity is mainly due to dissociation of intercalated water molecules coordinated to cations. Then, a variety of organic reactions that are catalyzed by strong and hazardous mineral acids such as etherification, esterification, and rearrangement/isomerization were successfully carried out with MMT catalysts.²⁶ On the other hand, the Lewis acid is located in the octahedral sheets of MMT. Then, additions such as Diels–Alder cycloaddition²⁹ and Michael reaction²⁶ that are catalyzed by Lewis active sites can be efficiently promoted by cation-exchanged MMT.

Accordingly, MMT can be of great interest in the case of FA polymerization for two main reasons. First, the use of natural clays as heterogeneous green catalyst would allow efficient replacement of the above-mentioned hazardous catalysts. In addition, the dual-acidic character of MMT could catalyze both condensation and addition during FA polymerization. To our knowledge, no studies have been devoted to FA polymerization under a dual Lewis/Brönsted catalysis. Only one study has been dedicated to the preparation of PFA in the presence of MMT.³⁰ The authors successfully exfoliated MMT layers into the polymeric matrix leading to PFA nanocomposites with improved thermal stability. However, the catalytic role of MMT was not discussed.

In the present study, sodium MMT (Na-MMT) and an organically modified MMT (Org-MMT) are used to evaluate their catalytic effect on FA polymerization. For the first time, special attention is given to improve understanding of the catalytic role of MMT on condensations and branching steps occurring during FA polymerization. This represents a very important issue to elaborate fully biobased green polymers using natural clays as new green catalysts. In analogy with biobased catalysts, MMT could be called “geo-based” catalysts. For this purpose, the synergies and complementarities obtained from model-free kinetic analysis and chemorheological analysis of FA polymerization under Org-MMT or Na-MMT catalysis are discussed. The influence of alkylammonium cations (the MMT organic modifier) on polymerization pathways is highlighted by separately using this primary ammonium cation as a homogeneous catalyst. Behind this strategy, the idea is to separately evaluate the activity of the Brönsted acidic site in the presence of alkylammonium cations and the activity of the Lewis acidic site in the presence of Na-MMT and try to highlight the possibility of dual catalytic behavior in the presence of Org-MMT. Polymerization in confined interlayer spaces of MMT leading to the exfoliation process might play a role in the overall kinetic pathway; this part is also discussed.

2. EXPERIMENTAL SECTION

2.1. Materials. Furfuryl alcohol (FA) was supplied by TransFurans Chemicals bvba (Belgium) and was used as received (purity >98%). Organically modified montmorillonite (Org-MMT), obtained by exchange of MMT counterions with octadecyl ammonium cations, was supplied from Nordmann, Rassmann GmbH (Nanomer I30E). Na-MMT (Montmorillonite K10) and octadecyl ammonium chloride (ODA) was obtained from Aldrich Chemical Co. Either Na-MMT or Org-MMT were mixed in FA under vigorous mechanical stirring at a weight ratio of FA/Na-MMT = FA/Org-MMT = 100/2. To determine the pH, 50 wt % aqueous solutions were prepared by weighing the respective amount of FA or FA/Org-MMT mixtures and deionized water in small vials. The pH of FA and

FA/Org-MMT aqueous solutions was 6 and 4.3, respectively. The FA/ODA weight ratio was fixed at 100/1.47 to get the same pH value obtained with the FA/Org-MMT system.

For the DSC and chemorheological experiments, the FA/Org-MMT, FA/ODA, and FA/Na-MMT mixtures were used without addition of water. Considering the stoichiometry of the reaction, the polymerization yield was deduced from thermogravimetric measurements and was ~75% in each case.

2.2. Polymerization of FA under Org-MMT, ODA, or Na-MMT Catalysis. The complete polymerizations of the three above-mentioned systems were followed by differential scanning calorimetry (DSC) and dynamic rheometry. To evaluate the kinetics of these complex polymerization pathways, the DSC curing data were computed using an advanced isoconversional method.

DSC Measurements. DSC experiments were made on a Mettler-Toledo DSC 823^e equipped with STAR software. Computations were performed using both internally written kinetic software that was regularly upgraded³¹ and “advanced model-free kinetics” STAR software. Temperature, tau lag, and enthalpy calibrations were performed using indium and zinc standards. Volatilization of the polycondensation byproduct occurs during the curing of the different mixtures, and consequently, high-pressure stainless steel crucibles were used instead of the usual aluminum crucibles because they can withstand vapor pressure up to 15 MPa. Samples of approximately 10 mg were placed into sealed pans. The DSC measurements have been conducted during polymerizations of FA/Org-MMT, FA/Na-MMT, and FA/ODA systems at the heating rates of 1, 2, 4, and 6 K·min⁻¹.

Chemorheological Analysis. Rheometrical measurements were conducted in oscillating mode with parallel plate geometries (40 mm diameter and 1 mm gap) on a Bohlin C-VOR rheometer with strain convection heating. The linear viscoelastic range of the material at its liquid and solid state has been evaluated by a strain sweep to determine the optimum deformation to measure complex modulus during the polymerization process. Measurements were carried out in auto stress mode with a frequency of 1 Hz and a deformation of 0.05%. Polycondensation reaction is accompanied by a water release leading to the formation of empty spaces between the plates. Due to this modification of geometry during experimentation, the measured modulii will be interpreted here more as relative values than absolute ones.

Theoretical Calculations. The rate of reactions is commonly described by the following equation:^{32,33}

$$\frac{d\alpha}{dt} = A \exp\left(-\frac{E}{RT}\right) f(\alpha) \quad (1)$$

where $(d\alpha)/(dt)$ is the reaction rate, α is the conversion degree, t is the time, T is the temperature, $f(\alpha)$ is a function used to describe the reaction model, E is the activation energy, A is the pre-exponential factor, and R is the gas constant.

The overall reaction rate is generally determined by the rates of both chemical reaction and diffusion processes.³⁴ Diffusion control becomes operative if the characteristic time of relaxation of the reaction medium exceeds the characteristic time of a chemical reaction. According to Debye,³⁵ the relaxation time for a molecule in a viscous medium is directly proportional to the viscosity. The effective characteristic time of a process is the sum of the characteristic time of chemical reaction $k(T)^{-1}$ and the characteristic time for reactants to diffuse in a viscous medium $k_D(T)^{-1}$, where $k(T)$ and $k_D(T)$ are

the reaction and diffusion rate coefficients. By the law of the addition of kinetic resistances,³⁴ the characteristic times can be replaced with the reciprocal rate constants, so that the effective rate coefficient can be written as the sum $k_{\text{ef}}(T)^{-1} = k(T)^{-1} + k_{\text{D}}(T)^{-1}$. Then, applying the isoconversional principle^{33,36} we obtain the apparent activation energy, E_{α} (for more details, see S. Vyazovkin et al.³⁷)

$$\begin{aligned} E_{\alpha} &= \frac{k(T)^{-1}E + k_{\text{D}}(T)^{-1}(RT + E_{\eta})}{k(T)^{-1} + k_{\text{D}}(T)^{-1}} \\ &= \frac{k_{\text{D}}(T)E + k(T)E_{\text{D}}}{k(T) + k_{\text{D}}(T)} \end{aligned} \quad (2)$$

where E is the activation energy of the chemical reaction, E_{η} is the activation energy of the viscous flow, and $E_{\text{D}} = E_{\eta} + RT$.

Equation 2 suggests that, depending on the temperature, the apparent activation energy, E_{α} , may take values between E and E_{D} or between E and E_{η} because, at low temperatures, the term RT can be neglected ($E_{\text{D}} \approx E_{\eta}$). Furthermore, the E_{α} dependence should be different for the cures performed under different temperature ranges.

This equation was obtained by postulating an Arrhenius type of temperature dependence for viscosity according to Eyring's theory of viscosity. Applying an isoconversional method to thermoanalytical data requires the computation of a single value of the activation energy for each α value (E_{α}). If one uses non-isothermal measurements, this means that a value of the temperature that corresponds to a given conversion degree α ($T_{\alpha,i}$) has to be computed for each heating rate i . This can be achieved by using an appropriate interpolation algorithm. Thus, the temperature interval used for the computation of E_{α} is relatively narrow because it lies in between $T_{\alpha,i}$ and $T_{\alpha,f}$, where i and f denote, respectively, the first and last heating rate used (β_i, β_f) in the series of experiments. Then, this computation is performed over a very limited temperature domain [$T_{\alpha,i}; T_{\alpha,f}$] ≈ 10 °C, where this approximation can be considered as valid.

For multistep kinetics, the global value of α does not uniquely determine the composition of the sample. This ultimately causes E_{α} to vary with α that reflects the variation in relative contributions of single steps to the overall reaction rate. Revealing the dependence of the activation energy on conversion with the help of isoconversional methods permits not only the disclosure of the complexity of a process, i.e., in detecting multistep processes, but also assistance in identifying its kinetic scheme and gaining insight into their mechanisms.

An advanced isoconversional method has been developed in order to be applicable for any temperature program and was used in this study.^{36,38,39} A minimization procedure is repeated for each value of α to determine the E_{α} -dependence.⁴⁰ The apparent activation energy calculated by isoconversional methods is a global energy that reflects a change in the rate-determining step of the overall reaction that may include several chemical reactions (multistep kinetics) as well as physical transformations (evaporation, gelation, vitrification). These methods can take into account the change from a chemically controlled reaction to a reaction controlled by the change in viscosity or by diffusion. The mean of absolute relative error on E_{α} values is $\sim 15\%$ for $\alpha < 0.10$ or $\alpha > 0.90$ and $\sim 5\%$ for $0.10 < \alpha < 0.90$.⁴¹

This kinetic method was programmed on internally generated kinetic software already described.^{42,43}

2.3. Preparation and Characterization of PFA/Org-MMT and PFA/Na-MMT Materials. The FA/Org-MMT and FA/Na-MMT mixtures were slowly prepolymerized at 80 °C during 48 h under vigorous mechanical stirring. Then, the systems were post-cured from 125 to 155 °C during 4 h to obtain PFA/Org-MMT and PFA/Na-MMT. DSC runs conducted on the cured samples did not highlight any residual heat of polymerization, indicating that the obtained material was almost completely cross-linked.

XRD and TEM analysis were used to assess the dispersion of MMT layers in the PFA matrix. The TEM images were obtained from a Philips CM12 using an accelerator voltage of 120 kV. Before analysis, the samples were previously cut using an ultramicrotome. The inorganic components appear black/gray-colored on the micrographs. The X-ray diffractometer was a PANalytical operating at 30 kV and 20 mA. The X-ray source was a Cu K α radiation with a wavelength of 1.54 Å. Radial scans were recorded in the reflection scanning mode from 1° to 15° at 0.06°/min.

2.4. Treatment of Org-MMT and Na-MMT with FA for FTIR Analysis. The FA/Org-MMT and FA/Na-MMT mixtures were slowly prepolymerized at 80 °C during 2 h under vigorous mechanical stirring. At the end of prepolymerization, the two solutions exhibit black/brown coloration which means that polycondensation—leading to chromophore formation—has occurred. In each case, the Org-MMT or the Na-MMT was recovered by centrifugation immediately after prepolymerization. Each MMT sample was washed, respectively, three times with water and acetone under sonication in order to eliminate adsorbed compounds on outer MMT surfaces. These so-called Org-MMT_(FA-treated) and Na-MMT_(FA-treated), as well as the pristine MMT, were dried overnight at 60 °C under vacuum prior to FTIR analysis.

The FTIR spectra have been recorded on a Perkin-Elmer Spectrum BX II spectrophotometer. The attenuated total reflectance (ATR) mode was used to characterize both Org-MMT_(FA-treated) and Na-MMT_(FA-treated). The pristine Org-MMT and Na-MMT spectra were also recorded with the same experimental conditions. To increase the signal-to-noise ratio, a total of 64 scans were accumulated for each measurement at a spectral resolution of 4.0 cm⁻¹.

3. RESULTS AND DISCUSSION

3.1. Dispersion of Clay Layers during Polymerization.

In the forthcoming sections, the discussion will focus on how the clay influences the FA polymerization pathway. The present paragraph aims at investigating the dispersion state of the clay platelets in the matrix at the end of polymerization and to determine if FA and ensuing oligomers are effective dispersants for MMT layers.

Figure 1 presents the XRD patterns of the raw (Na-MMT) and organically modified clay (Org-MMT) and the corresponding PFA/Na-MMT and PFA/Org-MMT materials after polymerization. Na-MMT exhibits a (001) diffraction peak at $2\theta = 7.01^\circ$. The basal spacing calculated with the Bragg eq ($2d \sin \theta = n\lambda$) is $d_{001} = 12.6$ Å. The presence of the alkylammonium cation in Org-MMT shifts the peak position to lower angle ($2\theta = 4.12^\circ$; Figure 1b) evidencing an increase in the gallery basal spacing to $d_{001} = 21.4$ Å. If we consider that the thickness of one MMT layer is 10 Å,⁴⁴ it gives an available interlayer space of 2.6 Å and 11.4 Å for Na-MMT and Org-MMT, respectively. The XRD profile of PFA/Na-MMT shows a reduced diffraction peak at $2\theta = 5.39^\circ$ (16.7 Å) attesting for

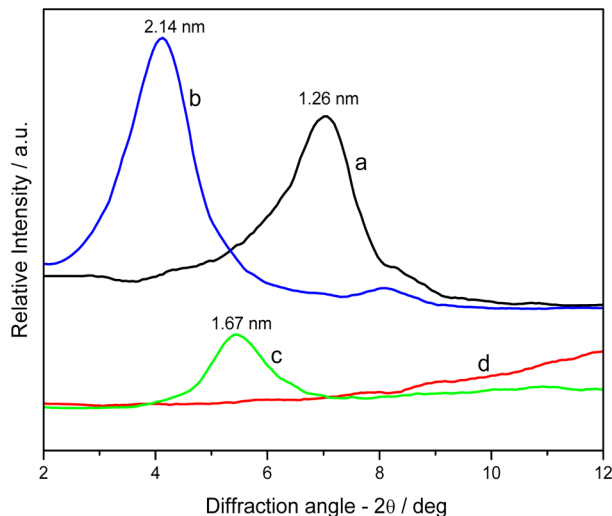


Figure 1. X-ray diffraction patterns of Na-MMT (a), Org-MMT (b), PFA/Na-MMT (c), and PFA/Org-MMT (d).

the presence of intercalated clay tactoids after FA polymerization. The expansion of layer basal spacing from 12.6 to 16.7 Å is due to intercalation of furanic units into the Na-MMT gallery. The reduced peak intensity also suggests partial exfoliation of clay layers. Concerning the PFA/Org-MMT system, the characteristic diffraction peak observed previously at $2\theta = 4.12^\circ$ for Org-MMT completely disappears, suggesting that the clay platelets are exfoliated. It indicates that furanic segments intercalate inside the MMT galleries and that the polymer chain growth tears the galleries apart leading to exfoliation of MMT layers. Such observations are in good agreement with the study of Pranger et al.³⁰ on the same system.

In order to get more information on the nature of the intercalated compound, FTIR has been applied to pure clays and to clays treated with FA. The evolution of the vibrational peaks after treatment of either Org-MMT or Na-MMT with FA would indicate the existence of cation exchange due to intercalation of furanic compounds between silicate layers. The corresponding spectra have been calculated applying the internal referencing method. All of the spectra were normalized to 1 at 1023 cm^{-1} , band assigned to the major absorbance of the Si–O stretching vibration in the layered silicate. Then, a subtraction was applied between clays treated with FA and pristine clay spectra. Figure 2 displays the resulting FTIR spectra in the $4000\text{--}400\text{ cm}^{-1}$ region obtained after the above-mentioned subtraction. The spectrum in Figure 2a shows major changes in band assignments corresponding to a strong decrease in the octadecylammonium absorptions. Peaks at 3236 and 3164 cm^{-1} which are attributed to ammonium NH_3^+ cations and those corresponding to the alkyl octadecyl bands at 2998 , 2830 , and 1464 cm^{-1} show negative deviations. It indicates that some ODA cations have been released outside clay interlayer spaces during FA treatment. In contrast, positive deviations are observed, which can be attributed to furanic cations. A significant positive peak can be observed at 1565 cm^{-1} , which is characteristic of the $\text{C}=\text{C}$ vibration, appeared by interconnection of a furan– CH_2 –furan group by condensation reaction. These results are in good agreement with those of Bertarione et al.⁴⁵ who observed for the first time the vibrational mode of distinct carbocationic species issued from FA polymerization in zeolite restricted spaces. By dosing NH_3 ,

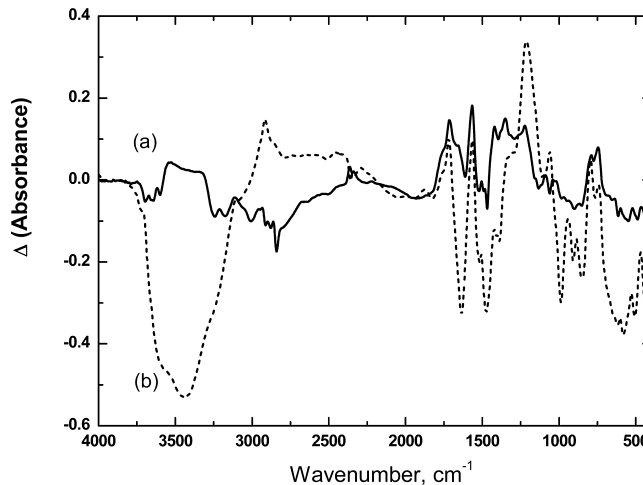


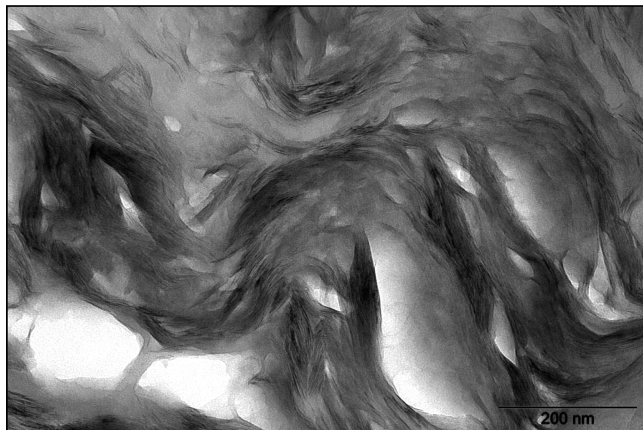
Figure 2. Difference of IR spectra: (a) $\Delta(\text{Absorbance}) = \text{Absorbance}_{(\text{Org-MMT/FA-treated})} - \text{Absorbance}_{(\text{Org-MMT})}$ (solid line); (b) $\Delta(\text{Absorbance}) = \text{Absorbance}_{(\text{Na-MMT/FA-treated})} - \text{Absorbance}_{(\text{Na-MMT})}$, in the region of $4000\text{--}400\text{ cm}^{-1}$ (dashed line).

which affects the FT-IR spectra of charged species, the authors demonstrated that the band near 1575 cm^{-1} is attributed to carbocationic species. As seen in Figure 2a, the formation of the diketone groups also appears with the positive deviation at 1710 cm^{-1} , which attests to hydrolytic ring cleavage during FA polymerization. These results indicate that, in the presence of Org-MMT, FA starts to polymerize, and the ensuing FA-based oligomers replace the octadecylammonium chains in the MMT galleries.

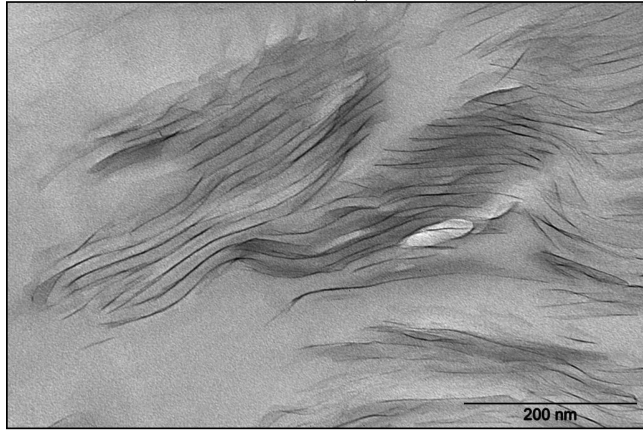
According to the spectrum in Figure 2b, the negative peak deviation of the free OH group at 3434 cm^{-1} together with the negative deviation at 1630 cm^{-1} is an indication of a strong decrease of water content in $\text{Na-MMT}_{(\text{FA-treated})}$. In parallel, we can note several positive deviations at 2915 , 1715 , 1565 , and 1215 cm^{-1} which indicate that furanic oligomers have intercalated between clay layers.

Figure 3a presents the TEM micrograph of a microtomed cross section of PFA/Na-MMT. The clay appears in the form of intercalated tactoids, and occasional exfoliated single platelets are observable. On the other hand, the PFA/Org-MMT exhibits a completely different morphology. As shown in Figure 3b, individual MMT layers are well-dispersed in the PFA matrix indicating that exfoliation has occurred. The average distance between platelets is higher than 15 nm. These TEM observations corroborate the XRD analysis.

3.2. DSC Analysis of FA, FA/Org-MMT, FA/ODA, and FA/Na-MMT Polymerization. Normalized nonisothermal DSC curves and the corresponding variation of conversion degree (α) obtained during the polymerization of FA/Na-MMT, FA/Org-MMT, and FA/ODA systems are shown in Figure 4. In each case, the total heat release of reaction, Q , and the maximum peak temperature (T_{\max}) were estimated from the DSC curves, and these thermoanalytical data are gathered in Table 1. The values obtained for neat FA, i.e., when polymerization is conducted with no catalyst, were also added in Table 1 (DSC scan not shown in Figure 4). It should be stressed that ODA, Org-MMT, and Na-MMT allow efficient promotion of the FA polymerization as suggested by the marked decrease in T_{\max} and increasing Q values compared to the noncatalyzed system (Table 1). However, differences are easily noticeable among the three systems. In the presence of



(a)



(b)

Figure 3. TEM micrographs of PFA/Na-MMT (a) and PFA/Org-MMT (b).

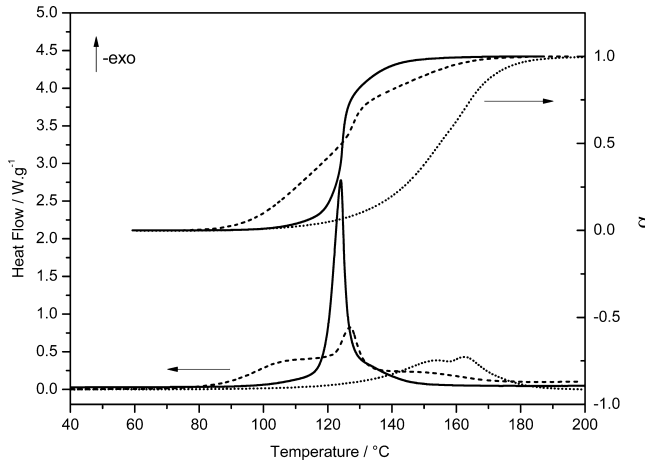


Figure 4. DSC data of the heat release (left-hand axis) and conversion degree (right-hand axis) during non-isothermal polymerizations at 2 K·min⁻¹ of FA/Org-MMT (solid line), FA/ODA (dash line), and FA/Na-MMT (dot line).

Na-MMT, which only contains a Lewis active site, the polymerization is promoted in comparison to single FA but starts at relatively higher temperature and present lower Q values compared to the systems containing Brønsted active site (i.e., FA/ODA and FA/Org-MMT). The unique presence of a Lewis acidic site in Na-MMT is not sufficient to obtain optimal catalysis and the same quantity of chemical reactions (i.e.,

Table 1. pH of Reacting Mixtures before Polymerization, Total Heat Release of Reaction (Q), and Maximum Peak Temperature (T_{\max}) Obtained during Polymerization of the Different Systems at 2 K·min⁻¹

reacting mixture	pH before polymerization (measured in 50 wt % aqueous solution)	total heat release Q/ (J·g ⁻¹)	maximum peak temperature $T_{\max}/^{\circ}\text{C}$ at 2 K·min ⁻¹
FA	6	428 ± 20	292 ± 1
FA/Na-MMT	7.3	507 ± 20	162 ± 1
FA/Org-MMT	4.3	557 ± 20	124 ± 1
FA/ODA	4.3	624 ± 20	126 ± 1

condensation + cross-links) that is reflected in lower Q values. Better results are obtained with systems containing a Brønsted acidic site, i.e., FA/ODA and FA/Org-MMT. However, it should be noted that the initiation of FA/ODA polymerization starts at lower temperature compared to FA/Org-MMT. This result seems logical, because in the case of the FA/ODA system, the early stage of polymerization will be initiated by the Brønsted acidity due to free ODA cations. For the FA/Org-MMT, the ODA cations are in this case intercalated between the clay layers. These cations are not able to initiate polymerization because they are stabilized by the extended anionic layers of MMT. It would explain why the initial stage of polymerization is retarded in the presence of FA/Org-MMT. In this case, initiation of polymerization could be attributed to a small fraction of Lewis active sites located on the outer surface of MMT layers, which are able to generate carbeneum centers on hydroxymethyl groups of FA. However, as soon as the polymerization is initiated, the reaction rate of FA/Org-MMT increases very rapidly and becomes faster than that of the FA/ODA system (Figure 4). We can note that Na-MMT do not lead to such an acceleration. Then, the acceleration observed in FA/Org-MMT could be a consequence of dual catalytic behavior from the Brønsted + Lewis active site. It would necessarily imply that small furanic cationic species have intercalated in interlayer spaces. This is confirmed by observation of exfoliated structures after polymerization (Figures 1 and 2) and by FTIR measurements (Figure 3).

3.3. Chemorheological Analysis of FA/Org-MMT, FA/ODA, and FA/Na-MMT Polymerization. Parallel plate rheometry is a common technique to characterize the curing behavior of thermosets. We applied this technique to the systems presently studied having in mind that rheometric measurements of the entire polycondensation process (i.e., from liquid state to glassy state) is difficult to investigate, because foaming, volatilization, and fast viscosity variations occur during curing. Figure 5 shows the evolution of storage modulus (G') with temperature for the FA/Org-MMT, FA/Na-MMT, and FA/ODA systems. It is worth noting that a low shear strain (0.05%) was chosen to give reliable data in the solid state, and then, G' and G'' values in the liquid state are sometimes out of the linear viscoelastic response of the material. Then, for the FA/Org-MMT and FA/Na-MMT systems, we will not consider the $G'-G''$ crossover—which is not clearly observed here—as the gel point. We will rather consider the intermediate plateau situated after gelation and before vitrification. This intermediate plateau will be referenced here as a postgel stage.

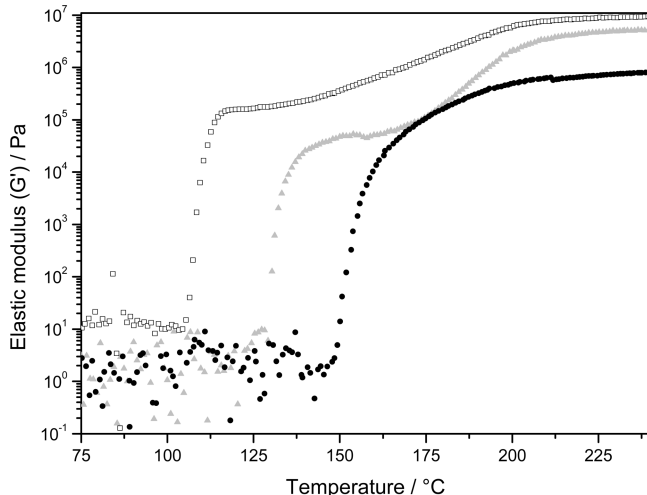


Figure 5. Variation of elastic modulus (G') during non-isothermal cure at $2\text{ }^{\circ}\text{C min}^{-1}$ of FA/Org-MMT (open squares), FA/ODA (solid circles), and FA/Na-MMT (solid gray triangles).

For the reacting mixtures containing MMT (FA/Na-MMT and the FA/Org-MMT), the increase of G' from the liquid state to the fully cross-linked glass follows three main steps. First, G' increases very quickly and reaches an intermediate plateau around 10^5 Pa . For these reacting systems, the onset of the postgel stage can be associated with the onset of diffusion control of the overall reaction rate. In the postgel stage, the molecular mass of reacting system is divided between a gel fraction and a sol fraction.⁴⁶ In a homopolymerization process such as FA polymerization, the sol fraction is composed of oligomers exhibiting different sizes. For the FA/Org-MMT and FA/Na-MMT, the onset of postgel stage can be taken at $T_{\text{postgel}} \sim 119\text{ }^{\circ}\text{C}$ and $\sim 150\text{ }^{\circ}\text{C}$, respectively, which correspond to DSC conversion degree of $\alpha_{\text{postgel}} \sim 0.13$ and ~ 0.40 , respectively. It appears clearly that, in the presence of Org-MMT, the system shows higher reactivity in good agreement with the above-mentioned DSC data. The onset of the postgel stage that can be associated with the onset of diffusion control starts at a very early stage ($\alpha_{\text{postgel}} \sim 0.13$), which corroborates the hypothesis of dual catalytic behavior of Org-MMT, i.e., Brønsted + Lewis. As demonstrated by FTIR measurements (Figure 3), the intercalation of some cationic species in MMT interlayer spaces will release the free ODA in the media. The presence of Brønsted acidic character leads to an increase of linear oligomers through condensation reactions, while the Lewis character preferentially promotes cross-linking between linear oligomers. Then, the gel fraction of FA/Org-MMT will expand rapidly at low conversion degree. The remaining sol fraction will be constituted mainly of residual monomers or low-molecular-weight oligomers. After the postgel stage, the storage modulus of either FA/Org-MMT or FA/Na-MMT re-increases slowly to reach a second and final plateau (Figure 5). This second step corresponds to the vitrification process, which results in a transition from the partly cross-linked to fully cross-linked material. The DSC heat flow measured during the vitrification process is very low (Figure 4) due to a dramatic reduction of chemical reactions as a consequence of diffusion control. On the contrary, the evolution of storage modulus during vitrification is well-marked. At this stage of polymerization, complementary information to the DSC measurements are given by rheometric data. As shown in Figure 5, the

modulus of FA/Org-MMT starts to re-increase at $T_{\text{vitrif}} \sim 130\text{ }^{\circ}\text{C}$ ($\alpha_{\text{vitrif}} \sim 0.82$), while FA/Na-MMT starts its vitrification process at $T_{\text{vitrif}} \sim 167\text{ }^{\circ}\text{C}$ ($\alpha_{\text{vitrif}} \sim 0.81$). However, they reach the glassy state approximately at $T_{\text{glassy-state}} \sim 213\text{ }^{\circ}\text{C}$ suggesting that the vitrification process of the FA/Org-MMT system occurs over a larger temperature range compared to FA/Na-MMT. The final cross-linking stage does not seem influenced by the nature of MMT. This is consistent with the fact that at this stage of reaction the cure kinetics is mainly driven by diffusion of unreacted species in the media.

As exhibited in Figure 5, the chemorheological behavior of FA/ODA differs from that of FA/Org-MMT and FA/Na-MMT. Its storage modulus starts to increase slowly between 140 and $150\text{ }^{\circ}\text{C}$, which corresponds to a very high DSC conversion degree of $0.80 < \alpha < 0.90$. A final and well-marked increase of FA/ODA modulus is observed above $150\text{ }^{\circ}\text{C}$. According to the results of DSC measurements (Figure 4, Table 1), we could expect that the chemorheological behavior of FA/ODA would be close to that of FA/Org-MMT. One must remember here that DSC reflects the heat release produced by all chemical reactions (i.e., condensation and cross-links), while the increase of G' is the direct consequence of the cross-link development. This explains the main differences observed between DSC and rheometric data. According to DSC data (Figure 4), we know that, at a very early stage of polymerization ($T < 115\text{ }^{\circ}\text{C}$), FA/ODA reacts more rapidly than FA/Org-MMT and FA/Na-MMT. This is obviously not reflected in rheometric data. Formation of the first oligomers by condensation reactions should not induce a detectable variation of viscosity. On the contrary, the cross-links develop at a slower rate in the FA/ODA system because the increase of modulus is shifted to higher temperature compared to FA/Org-MMT and FA/Na-MMT (Figure 5). Indeed, the ODA does not possess Lewis centers such as Org-MMT and Na-MMT. These results support the fact that Lewis active centers present in clays promote cross-links via electrophilic addition. It should also be stressed that rheometric measurements were done between two plates, i.e., in open conditions, while DSC was done in hermetically closed crucibles. The FA volatilization temperature is $\sim 170\text{ }^{\circ}\text{C}$ (under 1 atm). A previous thermogravimetric study has shown that, in addition to water, FA volatilizes during the whole polymerization process.⁴⁷ So at high temperature such as $130\text{--}140\text{ }^{\circ}\text{C}$, unreacted FA monomers still present in the FA/ODA system can volatilize partially outside the rheometric plates. It could explain why the final FA/ODA moduli in the glassy state ($\sim 10^6\text{ Pa}$) are slightly lower than those of FA/Org-MMT and FA/Na-MMT ($\sim 10^7\text{ Pa}$).

3.4. Kinetic Investigations of FA/Org-MMT, FA/ODA, and FA/Na-MMT Polymerization. In order to look for similarities and differences during the polymerization pathway of each reacting mixture, the E_{α} -dependencies were evaluated from multiple heating rate DSC data. The results are shown in Figure 6a,b. From these E_{α} -dependences, it can be unambiguously concluded that the non-isothermal acid-catalyzed polymerizations of the three analyzed samples follow multistep kinetics expressed by a strong dependence of apparent activation energy upon conversion. The compensation parameters were used to compute a value of $\ln A_{\alpha}$ for each value of E_{α} according to the procedure described elsewhere.^{33,48} The $\ln A_{\alpha}$ dependences are also plotted in Figure 6a,b for every system.

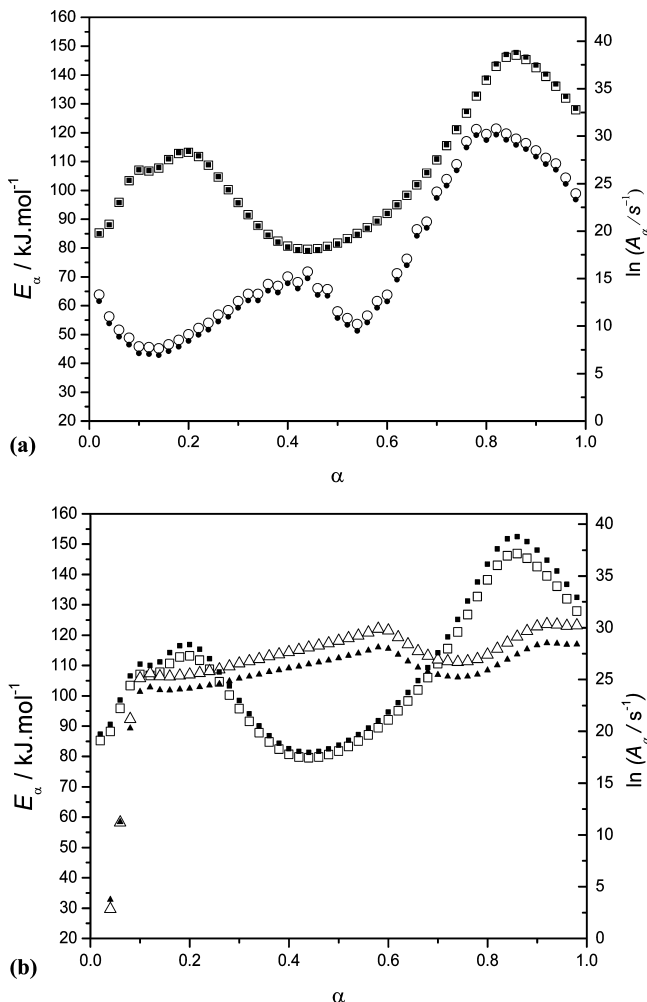


Figure 6. Variation in the effective activation energy (open symbols) and $\ln A_\alpha$ (solid symbols) with conversion obtained under non-isothermal conditions ($\beta = 1\text{--}6 \text{ K min}^{-1}$) for (a) polymerization of FA/Org-MMT (squares) and FA/ODA (circles); (b) polymerization of FA/Org-MMT (squares) and FA/Na-MMT (triangles).

For the homogeneous ODA catalysis, the obtained E_α intrinsic values and their variations with conversion (Figure 6a) are in very good agreement with those obtained in previous publications on FA polymerization catalyzed with another homogeneous catalysis (maleic anhydride).^{47,49} The outlined studies used the same kinetic approach and the attributions of the different mechanistic steps were previously done with the help of various spectroscopic techniques such as FT-IR and ¹³C liquid and solid-state NMR. Accordingly, comparison can be made and three different regions can be identified for the FA/ODA system spanning from low to high degree of conversion. First, a control by chemical reactions ($E_\alpha \rightarrow E$ when $\alpha \approx 0$, eq 2) including autocatalytic stage for $\alpha < 0.10$, then condensation and branching polymerizations for $0.10 < \alpha < 0.50$ and finally control by diffusion for $\alpha > 0.50$ ($E_\alpha \rightarrow E_D$ when $\alpha \approx 1$, eq 2). It should be mentioned in light of the previous kinetic analysis of FA polymerization that the decreasing shape of E_α -dependences around gelation ($\alpha \sim 0.50$) correspond to the region where diffusion control of unbranched small oligomer chains starts to become significant. This stage is immediately followed by a well-marked reincrease of E_α -dependence of FA/ODA to 100 kJ·mol⁻¹ (Figure 6a). The kinetic regime becomes

controlled by the mobility of longer chains and diffusion encounters a larger energetic barrier due to the cooperative nature of the motion, leading to higher E_α values. During the vitrification process ($\alpha > 0.85$), the curing rate becomes controlled by diffusion of small unreacted functions still present in the medium that is associated with a decrease in E_α -dependence of FA/ODA.

On the other hand, the FA polymerization conducted under heterogeneous Org-MMT or Na-MMT catalysts presents some differences with the FA/ODA reaction pathway. As shown in Figure 6a,b, the E_α -dependences of MMT-based systems are shifted to higher values compared to the homogeneous ODA system. One should remember that activation energy and pre-exponential factor ($\ln A$) have opposite contributions to the reaction rate. Thus, increasing values of $\ln A$ will increase the reaction rate. As shown in Figure 6a, FA/Org-MMT has higher $\ln A_\alpha$ values than FA/ODA, which explains why FA/Org-MMT polymerizes faster. On the other hand, this result would indicate that the presence of intercalated and/or exfoliated MMT layers in the media increases the efficiency of collisions on the layer surface. This hypothesis was already demonstrated by several authors.^{48,50,52}

As stressed by Montserrat et al.,⁵³ the influence of MMT on cure kinetics is often limited^{53,54} and generally leads to decreasing^{55–58} values of activation energy as a consequence of MMT catalysis from its active sites or from the organophilic cations. It has to be emphasized that clay layers influence the diffusion. Recently, Alzina et al.⁴⁸ obtained increased values of diffusion activation energy for epoxy/amine systems containing MMT. In some cases, the higher activation energies found for polymer crystallization in the presence of MMT were attributed to the role of clay layers on diffusion.^{59,60} Examples of FA polymerization in confined spaces can be found in the literature. PFA/SiO₂ hybrid networks were prepared via a sol–gel process,^{61,62} and confinement effects induced by silica network play a major role in thermomechanical properties.⁶² Bertarione et al.⁴⁵ studied the FA polymerization in protonic Y-zeolites. The authors proved by means of FT-IR, Raman, and UV-vis spectroscopies that the reduced reaction rate induced by the restricted spaces in zeolite channels allows the formation of oligomeric intermediates. The carbocationic character of these intermediates was clearly demonstrated.

The problem of FA polymerization in confined spaces is also applicable to the present study. When polymerization takes place in MMT interlayer galleries, the available space is limited to approximately $\sim 11.4 \text{ \AA}$ for Org-MMT and $\sim 2.6 \text{ \AA}$ for Na-MMT. These values are even lower than the supercage diameter of about 13 \AA found in zeolites.⁶³ It is noteworthy to remark that Org-MMT and Na-MMT can be destructured during polymerization due to intercalation of reagents, which generally leads to progressive exfoliation of clay layers. This is not the case with zeolites. So, the cleavage of the Org-MMT and Na-MMT layers occurring during polymerization (Figures 1 and 2) makes a positive contribution to the polymerization rate.

The E_α -dependence of the three systems was computed as a function of temperature (mean temperature over heating rates) as shown in Figure 7. Among the three systems, the FA/Org-MMT polymerizes more rapidly, i.e., over a shorter temperature range. However, the initiation of FA/Org-MMT and FA/Na-MMT polymerization is shifted to a higher temperature compared to that of ODA as shown in Figure 7. As suggested earlier, some furanic carbocation centers are probably formed by

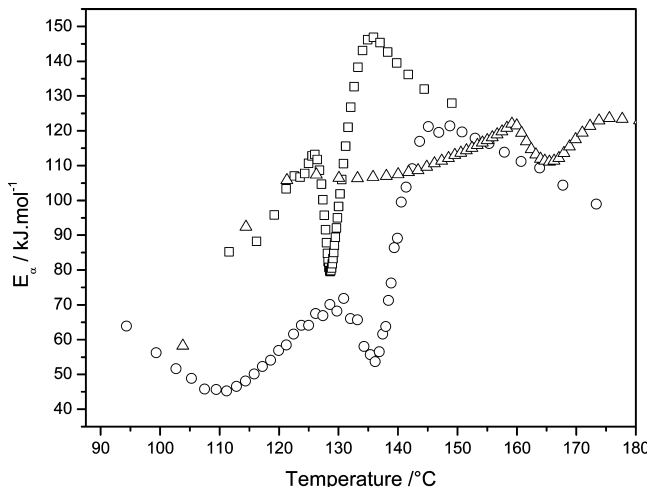


Figure 7. Variation in the effective activation energy with temperature obtained under non-isothermal conditions ($\beta = 1\text{--}6 \text{ K min}^{-1}$) for polymerization of FA/Org-MMT (squares), FA/ODA (circles), and FA/Na-MMT (triangles).

the presence of Lewis active sites on outer MMT surface or after intercalation of FA monomers directly in MMT interlayer spaces. It confirms that, in the presence of Org-MMT, the ODA cations are ionically bound to the clay and cannot promote the initial formation of carbocationic centers as in the case of FA/ODA. According to previous studies,^{64,65} adsorption and intercalation of organic species in interlayer spaces are complex mechanisms driven by van der Waals and Coulomb interactions. As shown previously by means of FTIR measurements, carbocationic species intercalate by cation exchange with ODA or Na^+ . The intercalated furanic carbocation centers will be stabilized between the extended anionic layers of MMT. Both intercalation and stabilization of carbocation centers in MMT interlayer spaces would explain why both FA/Org-MMT and FA/Na-MMT start to react at higher temperature compared to FA/ODA (Figure 4 and Figure 7).

If we look in more detail at Figure 6, some specific trends can be attributed to the presence of MMT layers at each step of polymerization growth. The E_α values of FA/Org-MMT increase rapidly at very early stages of polymerization (for $0.02 < \alpha < 0.20$). Such a profile is typical of independent or consecutive reactions.³⁶ The FA/ODA and FA/Na-MMT systems exhibit the same increasing behavior, respectively, for $0.10 < \alpha < 0.40$ and $0.10 < \alpha < 0.60$. This means that condensation and first branching reactions occur for the FA/Org-MMT system over a shorter conversion range leading to the gelled state at a very low extent of conversion. Compared to other systems, the control by diffusion of small oligomers becomes consequently rate-determining at early stages as suggested by the decreasing shape of the FA/Org-MMT dependence for $0.20 < \alpha < 0.40$ (Figure 6). This decrease in E_α values is well-correlated with the onset of postgel stage ($\alpha_{\text{postgel}} \sim 0.13$) deduced from rheometric data (Figure 5). The correlation obtained between chemorheological and model free kinetic analysis proves that Org-MMT behaves as an unconventional heterogeneous catalyst for FA polymerization because it contains both Brönsted and Lewis active sites. After first intercalations, several free ODA cations are released outside the MMT galleries and become available in the media. The presence of this Brönsted acid leads to the formation of small linear oligomers rapidly. As a consequence of this peculiar

dual catalytic behavior, the postgel stage is reached at a lower degree of conversion (i.e., $\alpha \sim 0.13$) compared to FA/ODA and FA/Na-MMT.

It must be emphasized that E_α values attributed to condensation and first branching vary between 84 and 114 $\text{kJ}\cdot\text{mol}^{-1}$ for FA/Org-MMT ($\alpha < 0.20$) and between 90 and 120 $\text{kJ}\cdot\text{mol}^{-1}$ for FA/Na-MMT ($0.10 < \alpha < 0.60$). For the FA/ODA system, the E_α values attributed to the same reactions vary between 44 and 74 $\text{kJ}\cdot\text{mol}^{-1}$ for $0.10 < \alpha < 0.50$. This difference of $\sim 30 \text{ kJ}\cdot\text{mol}^{-1}$ between MMT-based systems and FA/ODA can be assigned to the energetic barrier necessary on one hand to intercalate carbocationic species between MMT layers and on the other hand to overcome the stabilizing effect induced by these anionic layers. It supports the hypothesis that intercalation and stabilization of carbocationic species between restricted anionic MMT layers is occurring.

The polymerization growth between MMT layers leads to progressive exfoliation or intercalation of clay platelets within the media as confirmed by XRD patterns (Figure 1) and TEM observations (Figure 2) on cured PFA/Org-MMT and PFA/Na-MMT. The exfoliation process should occur at relatively early stage and will also contribute to give higher E_α and $\ln A_\alpha$ values compared to FA/ODA. For FA/Org-MMT, both intercalation and progressive exfoliation of clay layers will release the whole free ODA cation in the media. This results in an autoacceleration of the FA/Org-MMT polymerization rate as shown in Figure 6 by the dramatic decrease of E_α values for $0.20 < \alpha < 0.45$. Such autoacceleration is not observed for FA/Na-MMT. The E_α values slightly continue to increase for $0.20 < \alpha < 0.60$. The Na^+ released outside the galleries during the intercalation will not promote polymerization. It means that the autoacceleration observed for FA/Org-MMT is attributed to the progressive release of ODA in the reactive media. The synergy of both Brönsted acidity from free ODA and Lewis active site located on MMT layers has a positive contribution to the FA/Org-MMT reaction rate compared to other systems which present each of these acidic characters independently.

Fu and Heinz⁶⁶ have proposed a thermodynamic model for dispersion of layered silicates in polymer matrices where the free energy of exfoliation is tuned by the cleavage energy of clay layers. The cleavage energy depends essentially on the nature of interlayer species, and reduced cleavage energies lead to easier exfoliation. Other studies^{65,67,68} based on combinations of molecular simulations and experimental data highlight the thermodynamically driven process of exfoliation, i.e., difference between initial and final states. However, no attempts have been proposed to describe the kinetic pathway of the MMT exfoliation process in polymers due to the complexity for simulating such a phenomenon. The difference of $30 \text{ kJ}\cdot\text{mol}^{-1}$ observed at early stage of polymerization between MMT-based systems and FA/ODA can be taken as an activation energy linked to the intercalation of reagents between clay layers and the progressive exfoliation. This indicative value agrees well with the difference of $30 \text{ kJ}\cdot\text{mol}^{-1}$ already found between epoxy/amine/MMT and neat epoxy/amine systems when diffusion becomes rate-determining.⁴⁸

For $0.45 < \alpha < 0.85$ (Figure 6a), the FA/Org-MMT dependence reincrases to $E_\alpha \sim 145 \text{ kJ}\cdot\text{mol}^{-1}$. This variation can be attributed to control by diffusion of longer polymer chains that need to move cooperatively in order to allow continuation of the cross-linking process. However, the energetic barrier associated with this stage is much higher for the FA/Org-MMT ($E_\alpha \sim 145 \text{ kJ}\cdot\text{mol}^{-1}$) than in the case of the other catalysts such

as Na-MMT ($120 \text{ kJ}\cdot\text{mol}^{-1}$) or ODA ($\sim 110 \text{ kJ}\cdot\text{mol}^{-1}$). The difference of $\sim 25 \text{ kJ}\cdot\text{mol}^{-1}$ between FA/Org-MMT and the other systems can be attributed to the energetic barrier needed to overcome restriction of molecular mobility linked to the presence of exfoliated silicate sheets in the furanic matrix. At this stage of reaction, the influence of chemical reactions on curing kinetics is minimized.⁴⁹ No further reactions implying MMT catalytic sites are likely to occur. For the FA/Na-MMT, the layers are not completely exfoliated (Figures 1 and 2), and reagents have less difficulty to diffuse away from the media in this case compared to FA/Org-MMT, which results in a lower energetic barrier for the final stages. The higher values of $\ln A_\alpha$ found for the final stage of FA/Org-MMT polymerization (Figure 6) show that efficiency of collision is enhanced in the presence of exfoliated clay layers.

4. CONCLUSIONS

In the present study, biomass-based FA was polymerized in the presence of either heterogeneous Org-MMT or Na-MMT. Studying the influence of MMT on FA polymerization is particularly interesting, because this polycondensation process is catalyzed by Brönsted or Lewis acidic site and cationic species are formed during polymerization. The organophilic ammonium cation (ODA) present in the interlayer space of Org-MMT was also used as homogeneous catalyst to draw clear conclusions on the specific role of the silicate clay.

The MMT layers are intercalated and/or exfoliated during polymerization as evidenced by XRD and TEM analysis. This indicates that FA is compatible with Org-MMT or Na-MMT and acts as an effective dispersant for MMT sheets. Additional FTIR spectroscopy measurements have been performed to confirm the cation exchange and the intercalation of furanic species between silicate layers.

To determine and analyze the influence of Org-MMT and Na-MMT on the complete curing of FA, we performed DSC and rheometric measurements. Isoconversionnal analysis was applied to obtain new insight into the kinetic pathway. All the data lead to the conclusion that the silicate clay significantly increases the reaction rate and plays a peculiar role in the FA polymerization pathway.

On one hand, intercalation of reagents between the clay layers shifts the initiation of FA polymerization to a higher temperature. As soon as reactive species have intercalated, the peculiar dual catalytic behavior of Org-MMT (presence of Brönsted + Lewis acid sites) leads to acceleration of the reaction rate, and the gelled state is reached at an early stage of polymerization. Such acceleration is not highlighted when ODA (i.e., Brönsted acidity) or Na-MMT (Lewis active site) is used independently as polymerization initiator.

On the other hand, the presence of silicate clay layers restricts the diffusion of reactive species within the media and increases the efficiency of collisions which is reflected by an increase of E_α and $\ln A_\alpha$ values compared to the homogeneous system (FA/ODA). In the diffusion-controlled part of reaction, the presence of exfoliated clay layers also generate higher energetic (E_α) and entropic ($\ln A_\alpha$) barriers when longer polymer chains need to move cooperatively to allow continuation of the cross-linking process.

AUTHOR INFORMATION

Corresponding Author

*E-mail: guigo@unice.fr. Tel: +334 92 07 65 31/Fax: +334 92 07 61 19.

Notes

The authors declare no competing financial interest.

ACKNOWLEDGMENTS

The authors wish to thanks Dr. Urs Joerimann, Dr. Franck Collas, and Laurent Zoppi from Mettler-Toledo Inc. for fruitful collaboration and scientific exchanges.

REFERENCES

- (1) Gandini, A. *Green Chem.* **2011**, *13*, 1061–1083.
- (2) Moreau, C.; Belgacem, M. N.; Gandini, A. *Top. Catal.* **2004**, *27*, 11–30.
- (3) Gandini, A.; Belgacem, M. N. *Prog. Polym. Sci.* **1997**, *22*, 1203–1379.
- (4) Gandini, A. *Polym. Chem.* **2010**, *1*, 245–251.
- (5) Oliva-Teles, M. T.; Delerue-Matos, C.; Alvim-Ferraz, M. C. M. *Anal. Chim. Acta* **2005**, *537*, 47–51.
- (6) Zhang, X.; Solomon, D. H. *Chem. Mater.* **1999**, *11*, 384–391.
- (7) Epmeier, H.; Johansson, M.; Kliger, R.; Westin, M. *Holzforschung* **2007**, *61*, 34.
- (8) Stamm, A. J. *ACS Symp. Ser.* **1977**, *43*, 141–149.
- (9) Van-Rhijn, W.; Hoydonckx, H. E.; Van-Rhijn, W. Method for modifying wood with substituted furan compound impregnating solution and its modified wood. WO2007147804; 2007; p 62.
- (10) Dao, L. T.; Zavarin, E. *Holzforschung* **1996**, *50*, 470–476.
- (11) Toriz, G.; Arvidsson, R.; Westin, M.; Gatenholm, P. *J. Appl. Polym. Sci.* **2003**, *88*, 337–345.
- (12) Dunlop, A. P.; Peters, F. N. *The Furans. American Chemical Society Monograph No. 119.*; American Chemical Society: Washington, D.C., 1953.
- (13) Choura, M.; Belgacem, N. M.; Gandini, A. *Macromolecules* **1996**, *29*, 3839–3850.
- (14) Montero, A. L.; Montero, L. A.; Martínez, R.; Spange, S. *THEOCHEM* **2006**, *770*, 99–106.
- (15) Wewerka, E. M. *J. Appl. Polym. Sci.* **1968**, *12*, 1671–1681.
- (16) Mokoena, T. T.; Ddamba, W A A; Keikothaile, B. M. S. *Afr. J. Chem.* **1999**, *52*, 73–78.
- (17) Milkovic, J.; Myers, G E; Young, R. A. *Cellul. Chem. Technol.* **1979**, *13*, 651–672.
- (18) Principe, M.; Ortiz, P.; Martínez, R. *Polym. Int.* **1999**, *48*, 637–641.
- (19) Philippou, J. L.; Zavarin, E. *Holzforschung* **1984**, *38*, 119–126.
- (20) González, R.; Martínez, R.; Ortiz, P. *Die Makromolekulare Chemie* **1992**, *193*, 1–9.
- (21) González, R.; Martínez, R.; Ortiz, P. *Makromol. Chem., Rapid Commun.* **1992**, *13*, 517–523.
- (22) Sugama, T.; Kukacka, L. E. *J. Mater. Sci.* **1982**, *17*, 2067–2076.
- (23) González, R.; Rieumont, J.; Figueiroa, J. M.; Siller, J.; González, H. *Eur. Polym. J.* **2002**, *38*, 281–286.
- (24) González, R.; Figueiroa, J. M.; González, H. *Eur. Polym. J.* **2002**, *38*, 287–297.
- (25) Nagendrappa, G. *Resonance* **2002**, *7*, 64–77.
- (26) Kaneda, K. *Synlett* **2007**, 999, 1015.
- (27) Giannelis, E. P. *Appl. Organomet. Chem.* **1998**, *12*, 675–680.
- (28) Ferris, J. P. *Phil. Trans. R. Soc. B* **2006**, *361*, 1777–1786.
- (29) Fraile, J. M.; Garcla, J. I.; Gracia, D.; Mayoral, J. A.; Tarnai, T.; Figueras, F. *J. Mol. Catal. A: Chem.* **1997**, *121*, 97–102.
- (30) Pranger, L.; Tannenbaum, R. *Macromolecules* **2008**, *41*, 8682–8687.
- (31) Sbirrazzuoli, N.; Girault, Y.; Elégant, L. *Thermochim. Acta* **1997**, *293*, 25–37.
- (32) Prime, R. B. In *Thermal Characterization of Polymeric Materials*, 2nd ed., Turi, E. A., Ed.; Academic Press: New York, 1997.
- (33) Vyazovkin, S.; Burnham, A. K.; Criado, J. M.; Pérez-Maqueda, L. A.; Popescu, C.; Sbirrazzuoli, N. *Thermochim. Acta* **2011**, *520*, 1–19.
- (34) Frank-Kamenetskii, D. A. *Diffusion and Heat Transfer in Chemical Kinetics*, 2nd ed.; Plenum Press: New York, 1969.

- (35) Debye, P. *Polar Molecules*; The Chemical Catalog Co.: New York, 1929.
- (36) Vyazovkin, S.; Sbirrazzuoli, N. *Macromol. Rapid Commun.* **2006**, 27, 1515–1532.
- (37) Vyazovkin, S.; Sbirrazzuoli, N. *Macromol. Chem. Phys.* **2000**, 201, 199–203.
- (38) Vyazovkin, S. *J. Comput. Chem.* **1997**, 18, 393–402.
- (39) Vyazovkin, S. *J. Comput. Chem.* **2001**, 22, 178–183.
- (40) Sbirrazzuoli, N.; Vincent, L.; Vyazovkin, S. *Chemom. Intell. Lab. Syst.* **2000**, 54, 53–60.
- (41) Sbirrazzuoli, N.; Vincent, L.; Mija, A.; Guigo, N. *Chemom. Intell. Lab. Syst.* **2009**, 96, 219–226.
- (42) Sbirrazzuoli, N.; Brunel, D.; Elegant, L. *J. Therm. Anal.* **1992**, 38, 1709–1724.
- (43) Sbirrazzuoli, N. *Macromol. Chem. Phys.* **2007**, 208, 1592–1597.
- (44) Drummy, L. F.; Koerner, H.; Farmer, K.; Tan, A.; Farmer, B. L.; Vaia, R. A. *J. Phys. Chem. B* **2005**, 109, 17868–17878.
- (45) Bertarione, S.; Bonino, F.; Cesano, F.; Damin, A.; Scarano, D.; Zecchina, A. *J. Phys. Chem. B* **2008**, 112, 2580–2589.
- (46) Pascault, J. P.; Sautereau, H.; Verdu, J.; Roberto, W. *Thermosetting Polymers*; Marcel Dekker, Inc.: New York, 2002.
- (47) Guigo, N. Biomass based Materials: Polymers, Composites and Nano-Hybrids from Furfuryl Alcohol and Lignin. Ph.D. thesis, University of Nice Sophia Antipolis, 2008.
- (48) Alzina, C.; Sbirrazzuoli, N.; Mija, A. *J. Phys. Chem. B* **2010**, 114, 12480–12487.
- (49) Guigo, N.; Mija, A.; Vincent, L.; Sbirrazzuoli, N. *Phys. Chem. Chem. Phys.* **2007**, 9, 5359–5366.
- (50) Vyazovkin, S., Private communication with Professor S. Vyazovkin from University of Alabama at Birmingham, 2008.
- (51) Li; Simon, S. L. *Macromolecules* **2008**, 41, 1310–1317.
- (52) Li, Q.; Simon, S. L. *Macromolecules* **2009**, 42, 3573–3579.
- (53) Montserrat, S.; Román, F.; Hutchinson, J. M.; Campos, L. J. *Appl. Polym. Sci.* **2008**, 108, 923–938.
- (54) Ivankovic, M.; Brnadic, I.; Ivankovic, H.; Mencer, H. *J. Appl. Polym. Sci.* **2006**, 99, 550–557.
- (55) Ton-That, M. T.; Ngo, T. D.; Ding, P.; Fang, G.; Cole, K. C.; Hoa, S. V. *Polym. Eng. Sci.* **2004**, 44, 1132–1141.
- (56) Yei, D.-R.; Fu, H.-K.; Chen, W.-Y.; Chang, F.-C. *J. Polym. Sci., Part B: Polym. Phys.* **2006**, 44, 347–358.
- (57) Bao, S.; Shen, S.; Liang, G.; Zhai, H.; Xu, W.; He, P. *J. Appl. Polym. Sci.* **2004**, 92, 3822–3829.
- (58) Becker, O.; Simon, G. P.; Varley, R. J.; Halley, P. J. *Polym. Eng. Sci.* **2003**, 43, 850–862.
- (59) Goodarzi, V.; Jafari, S.-H.; Khonakdar, H. A.; Monemian, S.-A.; Hässler, R.; Jehnichen, D. *J. Polym. Sci., Part B: Polym. Phys.* **2009**, 47, 674–684.
- (60) Durmus, A.; Ercan, N.; Soyubol, G.; Deligöz, H.; Kaşgöz, A. *Polym. Compos.* **2010**, 31, 1056–1066.
- (61) Müller, H.; Rehak, P.; Jäger, C.; Hartmann, J.; Meyer, N.; Spange, S. *Adv. Mater.* **2000**, 12, 1671–1675.
- (62) Guigo, N.; Mija, A.; Zavaglia, R.; Vincent, L.; Sbirrazzuoli, N. *Polym. Degrad. Stab.* **2009**, 94, 908–913.
- (63) Marra, G. L.; Fitch, A. N.; Zecchina, A.; Ricchiardi, G.; Salvalaggio, M.; Bordiga, S.; Lamberti, C. *J. Phys. Chem. B* **1997**, 101, 10653–10660.
- (64) Hackett, E.; Manias, E.; Giannelis, E. P. *J. Chem. Phys.* **1998**, 108, 7410–7415.
- (65) PospIsil, M.; Kalendová, A.; Capková, P.; SimonIk, J.; Valásková, M. *J. Colloid Interface Sci.* **2004**, 277, 154–161.
- (66) Fu, Y.-T.; Heinz, H. *Chem. Mater.* **2010**, 22, 1595–1605.
- (67) Sinsawat, A.; Anderson, K. L.; Vaia, R. A.; Farmer, B. L. *J. Polym. Sci., Part B: Polym. Phys.* **2003**, 41, 3272–3284.
- (68) Heinz, H.; Vaia, R. A.; Farmer, B. L. *J. Chem. Phys.* **2006**, 124, 224713–224719.